UC San Diego
UC San Diego Previously Published Works

Title

Time Cells in the Hippocampus Are Neither Dependent on Medial Entorhinal Cortex Inputs nor Necessary for Spatial Working Memory.

Permalink

Journal

ISSN

Authors

Sabariego, Marta
Schönwald, Antonia
Boublil, Brittney L
et al.

Publication Date

DOI

Peer reviewed

Time cells in the hippocampus are neither dependent on mEC inputs nor necessary for spatial working memory

Marta Sabariego[1], **Antonia Schönwald**[1], **Brittney L. Boublil**[1], **David T. Zimmerman**[1], **Siavash Ahmadi**[1], **Nailea Gonzalez**[1], **Christian Leibold**[2,3], **Robert E. Clark**[4,5], **Jill K. Leutgeb**[1], and **Stefan Leutgeb**[1,6,7,*]

[1]Neurobiology Section and Center for Neural Circuits and Behavior, Division of Biological Sciences, University of California, San Diego, La Jolla, CA 92093, USA

[2]Department Biology II, Ludwig-Maximilians-Universität München, Martinsried, Germany

[3]Bernstein Center for Computational Neuroscience Munich, Martinsried, Germany

[4]Veterans Affairs San Diego Healthcare System, San Diego, CA 92161, U.S.A.

[5]Department of Psychiatry, University of California, San Diego, La Jolla, CA, 92093, U.S.A.

[6]Kavli Institute for Brain and Mind, University of California, San Diego, La Jolla, CA 92093, USA

[7]Lead contact

SUMMARY

A key function of the hippocampus and entorhinal cortex is to bridge events that are discontinuous in time, and it has been proposed that mEC supports memory retention by sustaining the sequential activity of hippocampal time cells. We therefore recorded hippocampal neuronal activity during spatial working memory and asked whether time cells depend on mEC inputs. Working memory was impaired in rats with mEC lesions, but the occurrence of time cells and of trajectory-coding cells in the stem did not differ from controls. Rather, the main effect of mEC lesions was an extensive spatial coding deficit of CA1 cells, which included inconsistency over time and reduced firing differences between positions on the maze. MEC is therefore critical for providing stable and distinct spatial information to hippocampus, while WM maintenance is likely supported either by local synaptic plasticity in hippocampus or by activity patterns elsewhere in the brain.

Declaration of interests

The authors declare no competing interests.

INTRODUCTION

Memory systems can hold previously presented information online over retention intervals of many seconds by persistent neuronal activity over temporal gaps. Although such ongoing activity was originally conceptualized as consisting of single cells that remain active over the entire delay interval (Fuster and Alexander, 1971), subsequent work has shown that persistent representations for retaining items in working memory (WM) can also be achieved with time varying activity (Druckmann and Chklovskii, 2012). One such activity pattern consists of individual cells turning on and off at particular times within the sequence, and such cells have been referred to as time cells or sequence cells and have been described in the hippocampus (Allen et al., 2016; Gill et al., 2011; MacDonald et al., 2011; Pastalkova et al., 2008), medial entorhinal cortex (mEC) (Heys and Dombeck, 2018; Kitamura et al., 2015; Kraus et al., 2015) and prefrontal cortex (Baeg et al., 2003; Fujisawa et al., 2008; Liu et al., 2014; Tiganj et al., 2017; Yang et al., 2014). Furthermore, a major contribution of entorhinal cortex to bridging episodes separated in time is also supported by the finding that the mEC is critical for tasks with pronounced temporal components, including trace fear-conditioning (Hales et al., 2018; Suh et al., 2011) and delayed matching to sample (Robinson et al., 2017). In particular, the most direct link between entorhinal contributions to hippocampal temporal firing patterns and memory performance has been reported for transient optogenetic inactivation of mEC during the delay period of a WM task, which resulted in a disruption of CA1 time cells and in memory impairment (Robinson et al., 2017).

Despite the finding that time cells are found in the entorhinal cortex and hippocampus and that inputs from the entorhinal cortex are required for temporal organization of hippocampal activity (Robinson et al., 2017; Schlesiger et al., 2015), evidence for a direct support of memory over delays by the sequential activity of time cells has remained scarce. For example, in the study by Robinson et al., memory performance partially returned to baseline during control trials after inactivation, while time cells in CA1 did not revert to the temporally organized firing during the same trials. These results were interpreted as implying that mEC manipulations caused persistent changes in synaptic organization that altered neuronal firing patterns over minutes rather than seconds, which is consistent with the finding that hippocampal spatial firing patterns in CA1 were also persistently altered after transient mEC inactivation (Rueckemann et al., 2016). Furthermore, hippocampal time cells occur without any memory demand (Salz et al., 2016), sequence discrimination can occur without differential hippocampal activity in a repeated segment (Bower et al., 2005), and differential firing on common maze segments (i.e., trajectory coding) is more pronounced in tasks that do not depend on the hippocampus compared to hippocampus-dependent tasks (Ainge et al., 2007; Griffin et al., 2007). A further conceptual consideration is also that the continuation of sequential neuronal activation is likely time-limited by noise and thus not a mechanism that can support WM over extended delay intervals.

An alternate possibility by which the entorhinal cortex and hippocampus could support WM is by providing distinct neuronal activity patterns during the task phase when sensory inputs for the current context of the trial are available (Shapiro and Eichenbaum, 1999). The differential activity during presentation of the cues could then be maintained by synaptic

plasticity in local networks over the delay interval or be informative for other brain networks that support WM. In spatial alternation tasks, differential activity in advance of the delay period in each trial would occur on the return arms. To therefore distinguish whether mEC inputs to hippocampus contribute to WM by discriminating the spatial context or to the maintenance of sequential hippocampal firing patterns on common maze segments, we recorded single units and local field potentials (LFP) from the CA1 and CA3 area during a spatial alternation task in control and mEC-lesioned rats. To comprehensively identify possible mechanisms for memory maintenance over the retention interval, we tested a delay period of 10 seconds, over which time cells have been reported to bridge events, and a delay period of 60 seconds, which was chosen to identify circuit mechanisms when the capacity of ongoing sequential activity is likely exceeded.

RESULTS

Spatial WM was mEC dependent and improved with training in mEC-lesioned rats

The mEC is a hub that provides spatial and temporal information to the hippocampus (Hafting et al., 2005; Schlesiger et al., 2015). We therefore reasoned that a delayed spatial alternation task, which requires spatial memory retention over time and depends on hippocampal function (Ainge et al., 2007), likely also depends on mEC function. To confirm a critical role of mEC, we performed mEC lesions and trained animals to perform an alternation task on a figure-8 maze (Figures 1A and S3A). In the alternation task, rats ran down a center arm and turned left or right before returning to the base of the stem, where they were delayed for either 10 s or 60 s, or as a control, continued without a delay. On the next trial, they had to choose to turn in the opposite direction from the one during the previous trial to receive a reward. As reported for rats with hippocampal lesions in a similar task (Ainge et al., 2007), mEC-lesioned rats (n = 7) were not impaired in the continuous version of the task. While mEC-lesioned rats performed worse than controls (n = 8) with 10 s delays only at the end of the testing phase (p = 0.010, Tukey's test) they made significantly more errors than controls throughout all the testing phases with 60 s delays (p = 0.0002, 0.0013 and 0.0037, Tukey's tests) (Figure 1B and Table S1). However, WM performance significantly improved with training in both mEC lesioned and control rats (Figure S3B and Table S3), plateauing for mEC-lesioned rats well above chance levels in both the 10 s and 60 s delay conditions (p = 0.0001 and 0.0124, respectively, one-sample t-test; Figure S3B). Our results thus show that mEC lesions resulted in a WM impairment, but also in partially spared memory, in particular in shorter delay conditions.

Combined lesions of the hippocampus and mEC resulted in a more severe and long lasting memory deficit than lesions of only mEC

Manipulations of mEC by lesion and inactivation have previously been shown to result in substantially deteriorated hippocampal spatial and temporal firing patterns (Hales et al., 2014; Miao et al., 2015; Robinson et al., 2017; Schlesiger et al., 2015), which raises the possibility that mEC lesions result in a loss of memory-related function of not only mEC, but via the loss of mEC inputs, also of the hippocampus. If this were the case, the retained WM in mEC lesioned rats could be mediated by brain areas other than mEC and hippocampus. However, if remaining hippocampal function in mEC lesioned rats continues

to at least partially support WM, hippocampal damage in addition to mEC damage should further exacerbate memory impairment. To distinguish between these possibilities, we performed combined mEC and hippocampus (mEC+H) lesions. These animals (n = 5) performed similarly to the control and mEC lesion groups during trials with no delay, consistent with the notion that neither the hippocampus (Ainge et al., 2007) nor mEC is critical for the continuous version of the task. However, with delays of either 10 s or 60 s, mEC+H lesions resulted in a much more pronounced memory impairment than mEC lesions (p < 0.0001, Tukey's tests; Figure 1B and see also Table S1). Moreover, no recovery was observed with mEC+H lesions, such that animals with combined lesions always performed at or below chance levels in both delay conditions (n.s., one-sample t-tests) (Figure 1B, S3, Table S3). To examine how the performance of rats with the mEC+H lesion could be below chance level, we analyzed whether these rats were prone to making strings of consecutive errors (Figure 1C). Such behavioral inflexibility was increased in rats with mEC+H lesions at longer delays (p = 0.0002, Tukey's test) but not in either control or mEC lesioned rats. Taken together with the results from rats with selective mEC lesions, the results from the mEC+H lesions suggest that the hippocampus, when intact in an mEC-lesioned rat, can at least partially support spatial WM.

The mEC lesion extent was similar in rats with only mEC lesions and in rats with mEC+H lesions

To confirm that differences in performance between rats with selective mEC lesions and those with mEC+H lesions were a consequence of adding the hippocampal lesion and did not result from different lesion extents within mEC, we visualized any remaining neurons in the target of the lesion in cresyl-violet stained sagittal sections and used the Cavalieri method to quantify the lesion extent (Figure 1D, S1A-C and S2). In the mEC lesion group (n = 10), 93.0% of the total mEC volume was completely ablated (95.3% of layer II, 92.4% of layer III and 91.4% of deep layers) with the majority of the sparing in the most ventromedial extent of the mEC (Figures 1D and S1A), which projects predominantly to the ventral hippocampus (Hargreaves et al., 2005). The lesions were thus extensive and consistently included the complete dorsocaudal portion of mEC where grid cells and other spatially selective cells are found (Diehl et al., 2017; Hafting et al., 2005). In the group with mEC+H lesions, 93.8% of the total mEC volume was completely ablated (91.3% of layer II, 95.0% of layer III and 95.1% of deep layers), again with the majority of sparing in the most ventromedial extent of the mEC. No significant differences in mEC lesion extent were found between the mEC lesion and mEC+H lesion group (n.s., two-way ANOVA with control/ lesion groups and brain areas as factors). Damage to areas other than mEC was predominantly observed in parasubiculum (Figures S1C and S2B). In the mEC+H lesion group, hippocampal lesions were extensive and included all subregions and a substantial portion of the presubiculum (94.9% of CA areas, 92.9% of DG, 90.0% of subiculum and 78.9% of presubiculum; see Figure S2).

Hippocampal spatial firing patterns in the alternation task were more severely disrupted in the CA1 compared to the CA3 subregion

The finding that mEC+H lesions resulted in a much more severe memory impairment than lesions of only the mEC suggests that the hippocampus contributes to spatial memory after

loss of mEC inputs. To identify hippocampal network mechanisms that could support the retained spatial WM, we compared the firing patterns of CA1 cells between control rats and mEC lesioned rats while rats performed the spatial alternation task. Because spatial deficits in CA1 after mEC lesions were previously reported to be substantial (Hales et al., 2014; Miller and Best, 1980; Schlesiger et al., 2015), we also examined whether CA3 spatial firing patterns depended on mEC inputs to the same extent as CA1 (n = 246 CA1 and 218 CA3 cells in 7 control rats; 233 CA1 and 359 CA3 cells in 10 mEC-lesioned rats).

We began our analysis by asking to what extent the hippocampal code for space was preserved across the entire figure-8 maze while lesioned rats performed the alternation task. For this analysis, we selected cells with a peak rate of > 2 Hz in at least one spatial bin, which included 72.4% and 67.8% of CA1 principal cells and 44.0% and 39.8% of CA3 principal cells in the control group and mEC lesion group, respectively. We first evaluated whether the loss of inputs from mEC to hippocampus resulted in changes of average and peak firing rates, but did not find differences for either measurement in CA1 or CA3 (n.s., KS test; Figure 2B). Next, we compared the spatial information of place fields between groups. Firing fields of CA1 pyramidal cells in the mEC lesion group had less spatial information compared to control CA1 cells (p < 0.0001, KS test; Figure 2AB). In contrast, CA3 pyramidal cells of mEC lesioned rats did not differ from CA3 control cells and CA1 control cells (n.s., KS tests). Consistent with the pronounced effect of the lesion on spatial information in CA1, CA1 place fields were larger in mEC lesioned rats compared to CA1 controls (p < 0.0001, KS tests; Figure 2B). While CA3 field size was also moderately increased in mEC-lesioned compared to control rats, the increase was less than in CA1 (p < 0.0001, two-way ANOVA; Figure 2B).

The hippocampal code for space could support spatial memory not only by firing at well-defined locations, but also by reliably firing at particular places. To examine the consistency of firing patterns between trials, we computed correlation coefficients between the spatial firing patterns of each trial with the spatial firing patterns of all other trials of the same type (i.e., between all pairs of right-turn trials and between all pairs of left turn trials) and averaged these values. No differences in spatial stability between control CA1 and control CA3 cells were found (n.s., KS test), while CA1 and CA3 cells from mEC-lesioned rats fired less consistently at the same location than those from control rats (p < 0.0001, KS test). However, mEC lesions had a more minor effect on the trial-by-trial correlations of CA3 cells compared to CA1 cells (p < 0.0001, two-way ANOVA; Figure 2B).

Spatial discrimination between return arms was more severely disrupted in CA1 compared to CA3

In spatial alternation, a subsequent correct choice depends on the accurate encoding of the preceding trajectory. Distinct representations of right and left return arms could therefore be particularly relevant to task performance. To measure the difference in firing patterns between one compared to the other side of the maze, we computed the spatial correlation between corresponding positions on the left versus right side of the maze [previously referred as "path equivalency"; Singer et al. (2010)]. To exclude effects from taking different turns at the choice point, we focused only on correct choices. We found higher correlation

coefficients for CA1 cells of mEC-lesioned compared to control rats (p < 0.0001, KS test), which indicated that cells in lesioned rats were more likely to fire at corresponding locations and showed reduced separation between left and right trajectories during the alternation task. In contrast, most active CA1 cells in return arms of control rats fired almost exclusively on only one side of the maze (Figure 3A). To confirm that the increased path equivalency in mEC-lesioned rats could not emerge by firing patterns overlapping by chance for cells with broader spatial firing in the maze, we performed shuffling of the right and left maze segments with respect to each other, and obtained correlation coefficients from shuffled data that were substantially below the observed ones (all p < 0.0001, KS tests, Figure S4).

Given that task-relevant information in the hippocampal CA1 area was substantially reduced in the return arms of mEC lesioned rats but that the hippocampus could nonetheless continue to partially support WM, we sought to identify whether hippocampal firing patterns remained intact in CA3. Consistent with the more minor effect on CA3 spatial coding when analyzing the entire maze (see Figure 2B), CA3 cells of mEC lesioned rats were also found to fire more exclusively on only one side of the maze and thus distinguished readily between left and right, similar to the pattern observed for control cells (Figure 3B).

Time cells during the 10 s delay period in control and mEC-lesioned rats did not distinguish between left-turn and right-turn trials

WM tasks have previously been found to display sequential neuronal activity during the delay period that discriminated between trial types. However, such activity was predominantly reported in an object-odor association task (MacDonald et al., 2011; Robinson et al., 2017) and in an alternation task that required continuous running during the delay period (Pastalkova et al., 2008). In our version of the task, animals were not forced to run during the delay and were tested with delay intervals of 10 s and 60 s. Without the requirement to continuously run in the alternation task, we found that only a low proportion of hippocampal CA1 and CA3 cells was active during the delay period in control as well as mEC-lesioned rats (Figure 4A and 5A). Because neuronal firing patterns that are informative about trial type should be most pronounced during correct trials, we focused on correct trials for our analyses. Despite the small proportion of active cells during the delay, we found that the firing patterns were sequentially organized over the 10 s delay, as previously reported for delay periods of similar length (MacDonald et al., 2011; Pastalkova et al., 2008; Robinson et al., 2017). However, the sequential firing patterns were not any more distinct between left-turn and right-turn trials than between blocks of trials of the same type, and sequential firing patterns were not deteriorated in animals with mEC lesions (n.s., two-way ANOVA with trial type and control/lesion group as factors; see Figure 4BC for statistics). Consistent with the uninformative left-right differences in sequential activity, we also found that there were no trial-type dependent rate differences when averaging firing rates over either the first 5 seconds or the second 5 seconds (all Mann-Whitney tests against shuffled values, n.s., Figure 4C).

Discontinuous events over longer retention intervals were not bridged by time cells

Previous studies that reported time cells used delays of up to 20 s (MacDonald et al., 2011; Pastalkova et al., 2008), but it is well established that hippocampus-dependent memories can

be retained for longer time periods. Analysis of firing patterns during the 60 s delay therefore afforded us the opportunity to test whether sequential activity patterns in the hippocampus are also the mechanism that is used over delay intervals that are longer than tested in previous studies of sequence activity. In 60 s delays, we found that neuronal activity patterns showed evidence for sequence coding during the initial few seconds (Figure 5B). However, omitting the first 10 seconds from the analysis of time bin correlations revealed that hippocampal firing patterns were no longer temporally organized for the remaining 50 s (Figure 5C insets), and these results did not differ between the control and mEC-lesion group (n.s., two-way ANOVA tests). Furthermore, we confirmed with additional analyses that the firing patterns of cells over the delay interval were not informative about the trajectory. First, by computing correlations for sequences within each 5-second interval we confirmed that sequential cell activity was either not observed or when observed (e.g., during the initial 5 s period) did not differentiate between left versus right trials (Figure S5AB and Table S4 for statistics). Second, we constructed population vectors in time intervals of 1 s length and trained a linear classifier to distinguish left and right turns based on the population activity (Figure 6A). The classifier was not able to detect trial type for either future or past trajectories in CA1 and only to a very minor extent in CA3 (Figure 6A). Finally, we compared firing rate differences for each 5-s segment of the delay interval between trial types and found that differences where only higher than for shuffled data during the first 5 s of the delay, but not for the remainder of the delay interval (Figure 6B). Neither sequential nor differential neuronal activity in the hippocampus was therefore observed for memory retention over the longer delay interval in either control or mEC-lesioned rats, and the population activity was not informative for decoding trial type.

Similarity of hippocampal activity during the 10 s delay and the first 10 s of the 60 s retention interval

Because we found evidence for sequential activity during the 10 s delay as well as over the first seconds in the 60 s delay, we tested whether these sequences were corresponding. A comparison between the sequences across the two different delays revealed that sequences within the 10 s delay were highly correlated to sequences over the first 10 seconds of the 60 s delay for CA1 cells as well as CA3 cells (Figure S5C). Correspondingly, we also found that most cells that were active during the 10 s delay were also active over the first 10 seconds of the 60 s delay (Figure S5D). Although our data revealed matching activity over the first 10 seconds of absolute time, it has also been reported that hippocampal cells can stretch or compress, such that the time period when they fire remains at a corresponding relative time within each interval (MacDonald et al., 2011). However, our analysis revealed substantially lower correspondence with relative compared to absolute time (all p < 0.001, Mann-Whitney tests, Figure S5C), consistent with our results that there are no detectable timed patterns after the initial 10 seconds in the 60 s delay.

Hippocampal cells that are active during the delay are partially corresponding to cells that are active in other maze segments

In consideration of the recent discovery that time cells in mEC that are active during immobility form a distinct subpopulation that did not overlap with mEC cells that were spatially modulated (Heys and Dombeck, 2018), we tested whether hippocampal cells that

were active when rats stopped during the delay were distinct from those that were active while running in other maze segments. In contrast to mEC cells, the fraction of CA1 and CA3 cells that were active during the delay as well as elsewhere on the maze was higher than expected (all p values < 0.01, Chi square tests, Figure S6). The same result was obtained even after further restricting the firing rates to periods of immobility by omitting the first 5 seconds in the delay, which is the period when rats had not yet slowed down. Again, more cells than expected were active in both the delay and elsewhere (all p values < 0.001, Chi square tests).

Trajectory-dependent firing differences in the maze stem were not reduced by mEC lesions

In addition to the delay zone, the stem is the part of the maze where animals have to retain or recall information about the previous trajectory to correctly decide on the next choice. Accordingly, hippocampal cells have been reported to fire differentially on the stem between trial types with different upcoming choices, even while the rat is in the same spatial location (Ainge et al., 2007; Bower et al., 2005; Ferbinteanu and Shapiro, 2003; Frank et al., 2000; Griffin et al., 2007; Johnson and Redish, 2007; Pfeiffer and Foster, 2013; Smith and Mizumori, 2006; Wood et al., 2000). Such trajectory-dependent differential hippocampal activity in advance of the turn could provide an internal representation that is used to support the appropriate upcoming goal choice. When analyzing differential activity of the cells that were active on the stem, we found that a large proportion of CA1 and CA3 cells in the control (CA1: 13 of 28 cells; CA3: 4 of 8 cells) and mEC lesion group (CA1: 9 of 20 cells; CA3: 10 of 15 cells) became differentially active, in particular in the most distal part, when the path of the animal started to deviate towards one side (see Figures 7 and S7 for comparison, and Table S2). In order to reduce a potential bias from the deviation of trajectories in the final segment of the stem we excluded the last 25 cm of the stem (up to 7.1 cm deviation in the final segment, 0.50–1.49 cm deviation in the remaining segments) from our analysis and found that the number of active cells dramatically decreased in both CA1 and CA3. Accordingly, trial type dependent firing only consistently differed from shuffled data when including (all p values < 0.05, KS tests), but not when excluding the final segment (Figure S7C).

DISCUSSION

Although mEC and hippocampus are both known to be critical for spatial and temporal components of memory, the circuit mechanisms for the processing of space and time remain incompletely understood. To investigate how mEC contributes to memory-related hippocampal function, we compared memory deficits between rats with combined mEC and hippocampus lesions and rats with only mEC lesions. Both lesion groups performed at control levels in a spatial alternation task without a delay, which is a task version that is known to not depend on the hippocampus and can likely be accomplished as a habit (Ainge et al., 2007). In versions of the spatial alternation task that include a delay and are thus hippocampus-dependent (Aggleton et al., 1986; Ainge et al., 2007; Dudchenko et al., 2000; Olton, 1979), rats with mEC lesions showed mild deficits in memory performance with 10 s delays and more pronounced deficits at longer delays. For both delays, memory performance was better preserved with mEC lesions than with combined mEC and hippocampus lesions.

These results suggests that mEC lesions disrupt memory-related hippocampal neural activity, but that there is, in rats with only mEC lesions, nonetheless spared task-relevant spatial and temporal hippocampal activity that can support WM performance above chance. We thus examined hippocampal neuronal firing patterns during the memory task, and found that loss of mEC inputs substantially reduced spatial coding in CA1, but to a lesser extent in CA3. In contrast, time cells over a 10-s delay were not diminished by the mEC lesion in either the CA1 or the CA3 subregion. However, in control and lesioned rats, time cells did not show distinct firing patterns between right-turn and left-turn trajectories. With 60 s delays, we did not detect trial-type dependent activity past a period of ~10 s, which further confirmed that differences in sequential hippocampal activity could not have been informative over the delay period. However, trajectory-dependent hippocampal activity re-emerged in both control and mEC lesioned rats along the stem of the maze. Taken together, these results suggest that partial memory deficits after mEC lesions are accompanied by less informative spatial firing patterns, which could hinder the encoding and updating of information during the return to the delay zone. In contrast, hippocampal firing patterns over the delay interval were neither found to be informative for memory performance nor depended on mEC inputs, which suggests that memory retention does not require continuously ongoing hippocampal activity during the delay interval.

While we did not find that cells in the delay zone were informative for spatial memory retention in delayed spatial alternation, previous studies that tested a potential contribution of the hippocampus and entorhinal cortex to WM have emphasized the coding properties of cells that are sequentially and differentially active during either the delay interval or on the maze stem. During these tasks phases, sensory information about the previous choice is no longer available, which implies that a trace of the previous experience needs to be held in memory. It has thus been suggested that hippocampal and entorhinal activity patterns over delay intervals are a key mechanism for maintaining the temporal continuity and for binding temporally discontinuous events (Eichenbaum, 2014; Kraus et al., 2015; MacDonald et al., 2011). Moreover, to be informative for subsequent choices, activation patterns of hippocampal cells would need to differ between trial types in WM tasks. However, such differential activity has been found to be particularly pronounced in tasks that are known to not be hippocampus-dependent or for which dependence on the hippocampus has not been explicitly tested (Ainge et al., 2007; Griffin et al., 2007; Hölscher et al., 2004; Ito et al., 2015; Lee et al., 2006; Wood et al., 2000). Paradoxically, for versions of spatial WM tasks which are hippocampus dependent, previous reports found that hippocampal CA1 activity during the delay or initial portion of the stem was not informative about the subsequent choice (Ainge et al., 2007; Ito et al., 2015). Although the occurrence of differentially active hippocampal cells on common maze segments is therefore well established, the necessity of such trajectory-dependent activity for memory retention in a hippocampus-dependent version is neither supported by previous findings nor by our findings.

A key difference between spatial alternation tasks without differential activity compared to those that reported differential activity is that those with differential activity typically required running over the entire delay period of up to 15 seconds (Pastalkova et al., 2008). The requirement to run resulted in sustained hippocampal theta oscillations over the entire delay, which could be a prerequisite for making the sequential activity contingent on the

preceding trajectory (Buzsaki and Moser, 2013). However, in numerous hippocampus-dependent tasks with delay intervals, ongoing theta states are not a prerequisite for memory retention (Ainge et al., 2007; Clark et al., 2002; Clark et al., 2000; de Lima et al., 2006; Duva et al., 1997; Hammond et al., 2004; Mumby et al., 1996; Prusky et al., 2004; Rampon et al., 2000; Takehara et al., 2003), which raises the question whether tasks without continuous running throughout the delay period may depend on different network mechanisms. Here we show that, in a task in which animals are not required to run over the delay, hippocampal cells are not differentially active between left-turn and right-turn trials except during the first few seconds. This suggests that hippocampal sequential activity over time is at best critical for memory retention over short intervals and that other mechanisms likely support working memory over longer intervals and in situations when theta states are not continuous, but when tasks critically depend on the hippocampus and entorhinal cortex. For example, awake sharp-wave ripples in hippocampus occur during brief periods of immobility and were found to be critical for future route planning and behavioral performance in spatial WM tasks (Girardeau et al., 2009; Jadhav et al., 2016; Sasaki et al., 2018).

In addition to observing that time cells were not informative for memory performance, we also found that time cells persisted in mEC-lesioned rats. Our results thus show that the specialized population of mEC time cells that is active during immobility (Heys and Dombeck, 2018) is not necessary for generating hippocampal time cell patterns during immobility over the delay interval. Furthermore, the hippocampal cells that were active during the delay were not a distinct population from those active in other parts of the maze, which is consistent with the findings that hippocampal cells can code for multiple features of a task (MacDonald et al., 2011; McKenzie et al., 2014). In addition, our finding of partially retained hippocampal time cells while memory performance is impaired appears to contradict a previous report that found CA1 time cells in an object discrimination task and that showed that sequential hippocampal activity as well as memory performance were diminished when mEC was optogenetically inhibited (Robinson et al., 2017). However, the transient mEC inactivation by Robinson et al. (2017) did not only result in a reorganization of hippocampal time cells during the period of mEC inhibition, but rather, the change in hippocampal firing patterns also persisted throughout trials in which the stimulation was not applied. Despite the disrupted sequence firing in no-stimulation trials, the manipulation did not cause a significant behavioral impairment in no-stimulation compared to baseline trials. Therefore, it appears that mEC inactivation resulted in a long-lasting reorganization of hippocampal sequential firing while hippocampus-dependent WM performance could at least partially recover in the absence of time cells. The partial recovery of memory but not of time cells can be considered as further evidence that time cells are not critical for WM performance.

If the function of hippocampus is not to provide persistent activity over the delay interval, how is memory retained and how do mEC and hippocampus contribute to memory retention? Although it is feasible that persistent activity over the delay could occur elsewhere in the brain, prefrontal cortex delay activity has been reported to correlate with memory retention only during learning but not in a well-trained WM task (Liu et al., 2014). Furthermore, in a delayed spatial alternation task, activity patterns in neither medial

prefrontal cortex nor nucleus reuniens were informative about the preceding trajectory during the second half of a 10–15 s long delay (Ito et al., 2015). In addition, prefrontal areas only compensated for hippocampal damage over short retention intervals (Lee and Kesner, 2003), and we show here that there is no compensation for combined mEC and hippocampus damage even with delays that are as short as 10 s. In contrast, memory partially recovered with mEC lesions, which suggests that degraded output from the hippocampus becomes progressively more useful with training. These findings thus suggest that the prefrontal cortex or other brain regions outside of the hippocampal formation can at least partially support task performance when at the minimum supplied with a spatial signal of low quality.

Together with previous studies (Ito et al., 2015; Lee and Kesner, 2003; Liu et al., 2014), our findings also raise the possibility that WM retention, in particular over longer intervals, may not be supported by persistent neuronal firing patterns. The encoding of a preceding trajectory would thus be more likely supported by other mechanisms, such as synaptic modifications within each trial throughout periods when cells are silent or not differentially active (Barak and Tsodyks, 2014; Ito et al., 2015; Mongillo et al., 2008; Stokes, 2015). With memory storage over the delay interval by modified synaptic connectivity, subsequent task-relevant activity would need to be reinstated, as indicated by the reemergence of trajectory-dependent activity in advance of the choice point (Figure 7; Ito et al., 2015). However, the reemergence of trajectory coding on the stem is even observed in mEC lesioned rats in which the substantially degraded CA1 activity on the return arms may have precluded that the trajectory is efficiently locally encoded. One possibility is therefore that the CA3 network is a site for plasticity during the task phase when the trajectory is encoded and that information about the preceding trajectory is forwarded from CA3 to CA1 after the end of delay. This is in agreement with the finding that CA3 excitation of CA1 neurons is strongest on the stem in the alternation task (Fernandez-Ruiz et al., 2017) and that CA3 slow gamma promotes recall of upcoming trajectories (Zheng et al., 2016). Moreover, CA3 to CA1 synaptic efficiency has been reported to increase after mEC lesions (O'Reilly et al., 2014), which could at least partially account for the mild behavioral deficit in mEC lesioned rats and for the substantially more pronounced deficit with combined lesions.

Taken together, our results indicate that the entorhino-hippocampal circuit does not necessarily contribute with time cell based mechanisms or any other type of persistent activity to working memory over delay intervals. Our results thus point to an alternate mechanism by which mEC could affect working memory. One possibility is that the contribution of mEC to WM consists of supporting the distinct encoding of the past choice by plasticity mechanisms, which can later support the reemergence of distinct activity in the local network during retrieval. Alternatively, mEC could provide spatially distinct firing patterns that can induce persistent or sequential activity elsewhere in the brain, such as in prefrontal cortex. However, the latter possibility is less likely for longer retention intervals, when compensation by prefrontal areas for the loss of hippocampal inputs has been shown to diminish (Lee and Kesner, 2003). Accordingly, we show that at increasingly longer retention intervals, which make memory performance more definitely hippocampus and mEC dependent, there is diminishing evidence for the manifestation of hippocampal time cells, suggesting that other mechanisms than time cells and related types of sequential activity support WM.

STAR METHODS

CONTACT FOR REAGENT AND RESOURCE SHARING

Further information and requests for resources and datasets should be directed to and will be fulfilled by the Lead Contact, Stefan Leutgeb (sleutgeb@ucsd.edu)

EXPERIMENTAL MODEL AND SUBJECT DETAILS

Subjects—All animal experiments were approved by the University of California, San Diego Institutional Animal Care and Use Committee and conducted according to National Institutes of Health guidelines. The subjects were 20 experimentally naïve, male Long–Evans rats weighing between 300 g and 350 g. Rats were housed individually on a reversed 12 h light/dark cycle. Behavioral testing and recording sessions were performed in the dark phase of the light-dark cycle. During periods of behavioral testing and recording, rats were food restricted and maintained at ~85 % of their ad libitum weight. The rats were divided into three groups, a group with nearly complete NMDA lesions of the medial entorhinal cortex (mEC; $n = 10$), a group with combined lesions of the mEC and the hippocampus (mEC+H; $n = 5$), and a control group (Control; $n = 9$). The animals were randomly assigned to one of the groups.

METHOD DETAILS

Surgical procedures—All surgeries were performed using aseptic procedures. Anesthesia was maintained throughout surgery with isoflurane gas (0.8–2.0 % isoflurane delivered in O_2 at 1 L/min) and buprenorphine (0.02 mg/kg) was administered as an analgesic. Animals were positioned in a Kopf stereotaxic instrument, and the incisor bar was adjusted until bregma was level with lambda. The bone overlying the target site was removed using a high-speed drill. The control group underwent these initial surgical procedures, but injections into the brain were not performed. The two experimental groups received excitotoxic lesions of either mEC or of mEC and hippocampus combined. For mEC lesions, NMDA was used as an excitatory analog of glutamic acid. NMDA (Tocris) was dissolved in aCSF (Harvard Instruments) to provide a solution with a concentration of 10 mg/ml and was injected at a rate of 0.1 μl/min using a 10 μl Hamilton (Reno, NV) syringe mounted on a stereotaxic frame and held with a Kopf model 5000 microinjector. The antero-posterior (AP) coordinate was measured from the anterior border of the transverse sinus, and the needle was inserted at medio-lateral (ML) ±4.6 mm with an angle of 22° moving from posterior to anterior. The syringe needle was lowered 5.2 mm from the dura and left in place for 1 min before the start of the injection. NMDA was injected into 8 sites [−5.2, −4.7, −4.2, −3.7, −3.2, −2.7, −2.2, and −1.7 mm dorsoventral (DV) from dura, 0.87 μl of toxin at each injection site], and was intended to damage the complete area of medial entorhinal cortex. The syringe needle was left in place for 1 min after the injection to reduce the spread of drug up the needle tract. For the additional hippocampal lesions in the combined lesion group, corresponding procedures were used with the following modifications. Instead of NMDA, ibotenic acid (Tocris) was dissolved in 1X PBS to provide a solution with a concentration of 10 mg/ml, pH 7.4. The toxin was injected into 18 sites (all coordinates are in mm, AP is relative to bregma, ML is relative to lambda, DV relative to dura, volume is in μl; AP −2.4, ML ±1.0, DV −3.5, 0.025 μl; AP -3.2, ML ±1.4, DV −3.1, −2.3, 0.05 μl; AP −3.2, ML ±3.0,

DV −2.7, 0.04; AP −4.0, ML ±2.5, DV −2.8, −1.8, 0.05 μl; AP −4.0, ML ±3.7, DV −2.7,0.04 μl; AP −4.8, ML ±4.9, DV −7.2, −6.4, 0.05 μl; AP −4.8, ML ±4.3, DV −7.7, −7.1, −3.5, 0.085 μl; AP −5.4, ML ±4.2, DV −4.4, −3.9, 0.05 μl; AP −5.4, ML ±5.0, DV −6.6, −5.9, −5.2, −4.5, 0.12 μl) on each side of the brain and was intended to damage the dorsal and ventral hippocampus. After completion of the injections, the skin was sutured, and the animal was allowed to recover from anesthesia on a water-circulating heating pad. All animals received postoperative care for at least 5 days after surgery.

After an interval of at least 9 weeks to allow for recovery and initial behavioral testing, all animals of the mEC lesion and control groups underwent a second surgery to implant a fourteen-tetrode recording assembly. The second surgery used the same general procedures as the first surgery but tetrodes were implanted in the cortical area above the dorsal hippocampus instead of performing injections. The recording assembly consisted of 14 tetrodes that were each constructed by twisting four 17 μm polyimide coated platinum-iridium (90 %/10 %) wires. The electrode tips were plated with platinum to reduce the impedances to 200–300 kΩ at 1 kHz. The tetrodes were arranged into a bundle targeted to the hippocampus in the right hemisphere (AP: 4.0 mm, ML: ±2.8 mm).

Behavior

Apparatus.: Behavior was conducted in a T-maze that was modified to include return arms and thus had a figure-8 shape (Figure 1C). The maze was constructed from a series of interlocking grey hard plastic runways that were 10 cm wide and fitted with 2 cm tall ridges of the same material on each side. The center runway that forms the stem of the figure-8 maze was 150 cm long and 10cm wide, as were the right and left return arms. A 101 cm long crosspiece connected the center arm to the right and left return arms at the top and at the bottom of the maze. One automatic and one manual barrier were used to interpose a delay interval between some of the trials. The delay zone was at the base of the center arm and 25 cm long. Food-rewards (chocolate sprinkles) were delivered at the distal ends of each of the top arms after the animals made a correct choice. The figure-8 maze was elevated 50 cm above the floor and positioned within an open environment with prominent and constant visual cues. A light source in a corner of the room (approximately 1 meter from the maze and 2 meters from the sleep chamber) kept the environment dimly illuminated.

Behavioral Task.: Before the beginning of the behavioral training, rats were given 4 weeks to recover from the lesion surgery. At the start of the training, rats were handled, were given chocolate sprinkles in their home cages for three days, and were familiarized with the room where the testing would take place by allowing them to freely explore the maze for 10 min with chocolate sprinkles scattered over the maze ("habituation day"). The next day, the first stage of testing began by placing the rat at the base of the center arm of the figure-8 maze. During this stage, a barrier was used to force the rat to enter one of the two side arms where a reward was delivered. After consuming the reward, the rat was guided to return to the base of the center arm and was allowed to run to the opposite connecting arm in a figure-8 pattern. The rat was prevented from retracing its route at any point. Each session was 20 min long or 30 trials, whichever came first. This procedure was repeated, using barriers on alternating arms until the animals ran the pattern consistently during two consecutive days.

In the second stage, the use of a barrier at the choice point was phased out and the rats were able to enter either arm each time they reached the end of the stem. However, they were rewarded only for running alternating arm entries in a figure-8 pattern, and they were prevented from retracing their steps at any point. Second stage sessions were 20 min long or 30 trials, whichever came first. Rats were trained to a criterion performance of at least 90% correct trials on two of three consecutive days. The third stage started once the rats reached this criterion and included trials with delay. In each daily session, rats received 30 trials grouped into three blocks of 10 trials (no delay, 10 s delay and 60 s delay for 7 mEC lesioned and 8 control rats, only these rats were used for behavioral analysis; no delay, 2 s delay, and 10 s delay for 3 mEC lesioned and 1 control rat, only the no delay and 10 s delay of these rats was used for analysis of hippocampal recordings). The order of the three blocks was pseudorandomized every day. During delay trials, as the rat returned to the base of the stem after the last trial of the previous block, two barriers were placed to confine the rat to a 25 cm zone at the base of the stem. At the end of the delay interval, the barrier that blocked access to the center arm was lowered and the rat was free to traverse the stem and make its next choice. After the rat made a choice and ate the reward, it returned to the delay zone on the center arm. This stage continued for 14 days.

Animals were then fed *ad libitum* for at least a week before the second surgery during which the recording assembly was implanted. During the recovery period from the second surgery, tetrodes were slowly advanced into the CA1 and CA3 areas of the hippocampus. After five days of recovery, rats started to run some trials without delays in order to get habituated to the recording cable that now connected the electrode assembly to the recording system. During tetrode advancement and recordings, the signals were preamplified with a unity gain headstage and were recorded with a data acquisition system with 64 digitally programmable differential amplifiers (Neuralynx, Tucson, AZ, USA). Spike waveforms above a threshold of 40–45 µV were time-stamped and digitized at 32 kHz for 1 ms. The rat's position was tracked at 30 Hz by recording the position of light-emitting diodes that were placed above the head. Local field potentials were acquired by recording one channel of each tetrode with the filters set to the 1–450 Hz band. As expected (Bragin et al., 1995) sharp wave ripples were not diminished by the mEC lesion and could therefore be used to guide electrode advancement into the cell layers in all rats. Recording in the figure-8 maze began when tetrodes were stably positioned in the CA1 and/or CA3 cell layer. Spikes and local field potentials were recorded during the alternation task and also while the rat was resting in a transparent holding chamber located in the same room for 1 hour at the beginning (sleep 1) and 1 hour at the end of each recording day (sleep2). Each animal ran one session per day for 6 to 12 days. Data collection and analysis were not performed blind to the conditions of the experiment.

Neurohistological methods and tetrode locations—At the end of the recording procedures, rats were administered an overdose of sodium pentobarbital and perfused transcardially with a phosphate buffered solution followed by 4% paraformaldehyde solution (in 0.1 M phosphate buffer). Brains were then removed from the skull and kept in a solution of 4% paraformaldehyde for 24 h before they were transferred to a 30% sucrose solution where they remained for an average of 48 hours. Sagittal sections (40 µm) were cut with a

freezing microtome beginning just lateral to the hippocampus and continuing medially through the hippocampus and mEC of each hemisphere. Every section was mounted and stained with cresyl violet to identify the hippocampal tetrode locations. Every fourth section was used to quantify the lesion extent with the Cavalieri method, as previously described (Hales et al. 2014). For MEC lesions, the volume of the spared tissue in the mEC layer II, mEC layer III, mEC deep layers, dorsal parasubiculum, and ventral parasubiculum was quantified. In the mEC-lesioned rats, cells in the superficial layers were either completely absent or, when small patches of cells were discernable, showed signs of disorganization and necrosis such as multipolar processes and fragmented nuclei (Schlesiger et al., 2018). Damage to brain areas other than the lesion targets and parasubiculum were not substantial, as previously reported (Hales et al., 2014). The percent of damage was calculated by normalizing the volume of spared tissue to the volume of controls with the formula below.

$$\% \ of \ damage = \left(1 - \frac{spared \ estimated \ volume}{average \ volume \ in \ control \ group}\right) \cdot 100$$

Tetrode trajectories through hippocampus were determined from 3D reconstruction of the sectioned tissue. Based on records of the systematic movement of tetrodes through the brain and the trajectory information, complemented by records of LFP profiles, tetrode locations on each recording day were assigned to either CA1 or CA3 regions.

QUANTIFICATION AND STATISTICAL ANALYSIS

Cell sorting and cell tracking.—Single units were manually sorted using MClust (version 3.5, written by A. David Redish; http://redishlab.neuroscience.umn.edu/MClust/MClust.html) and customized by Mankin et al. (2012). Clusters that persisted in the same region of parameter space throughout a whole session were accepted for analysis when the action potential amplitude/shape of spikes in each cluster were distinct from noise signals and remained inside the same set of cluster boundaries throughout the session. Recordings during rest periods (before and after the task) were used to confirm recording stability during the experiment and to identify hippocampal cells that were silent or fired at low rates during behavior. Up to three recording sessions per rat were considered for analysis and, while we tried to avoid double-counting cells by advancing tetrodes and/or by analyzing non-consecutive days, in some cases the same cells could have been recorded in more than one analysis day.

Cell classification.—Neurons were classified as putative interneurons versus putative principal neurons using a criterion applied to the relationship between spike ratio and spike rate (Csicsvari et al., 1999). Briefly, extracellular recordings of action potentials (spikes) were inverted resulting in an early upward peak (peak1) and a later downward peak (peak2). Mean spike ratios were calculated by dividing the absolute amplitude of peak 1 by the absolute amplitude of peak 2. The amplitude of the first peak is related to the rise time of the depolarization, and the amplitude of the second peak is related to the decay time of repolarization (Henze et al., 2000). Spike ratios are thus approximately equal to 1 for cells that have comparable rates of depolarization and repolarization, and interneurons rather than principal cells are known to have repolarization rates that are approximately equal to

depolarization rates. Therefore, cells that had spike rates below 15 Hz and spike ratios above 1 were considered putative principal cells and cells that had spike rates above 15 Hz and spike ratios below 1 were considered putative interneurons. Interneurons were not excluded from the analysis.

Rate maps—For the illustration of rate maps in Figure 2A, the figure-8 maze was divided into 5 cm x 5 cm bins. Spatial firing rate distributions were constructed by summing the total number of spikes that occurred in each location bin, dividing by the amount of time that the animal spent in that location, and then smoothing with a boxcar filter (Koenig et al., 2011). For quantitative analysis, the animal's path along the figure-8 maze was linearized, left-turn and right-turn paths were separated with each lap beginning and ending at the reward locations. Spikes rates were then calculated for each 5 cm-long segment along the maze tracks and smoothed with a one dimensional version of the boxcar filter. The linearized rate maps were used to determine peak rates, the spatial information, and rate differences between left and right trajectories. Only correct trials were analyzed.

Spatial correlation—The consistency of each cell's spatial firing pattern was measured by calculating, for each pair of left-turn trials and for each pair of right-turn trials, the Pearson's correlation between path segments at corresponding locations. Only correct trials were analyzed, and maze segments at the delay site were excluded. Pairwise comparisons in which the rates in all maze segments were less than 2 Hz were excluded. For each cell, the average correlation coefficient over all pairs of left-turn trials and the average over all pairs of right-turn trials was calculated, and the maximum of the two values was selected. The maximum was used so that cells with a place field on only one side of the maze would be assigned the correlation value from the trial type with the field. In addition to calculating spatial correlation coefficients between trials, we also averaged the firing rates over all left-turn trials and over all right-turn trials. These averages were used to calculate the spatial correlation between corresponding segments on the right and left side of the figure-8 maze. Maze segments on the stem were excluded when calculating the correlation between the two sides.

Correlation between time bins during the delay—In order to evaluate whether cells fired in a sequential manner during the delay, we computed Pearson's correlations between the firing rates in time bins over the delay interval. Each bin was 500 ms long and was smoothed by averaging over a 2500 ms window that was centered on the bin. Animals ran two blocks of 10 s delay trials and two blocks of 60 s delay trials in a daily session. Firing rate bins over the delay period in correct left-turn trials from the first block of 10 s delay trials were compared to firing rate bins in correct left-turn trials from the second block of 10 s delay trials. Similarly, firing rate bins in correct right-turn trials from the first block were compared to firing rate bins in correct right-turn trials from the second block. In addition, we also compared firing rate bins throughout the delay in correct left-turn trials with firing rate bins in correct right-turn trials of the same block. The same calculations were performed for blocks of trials with the 60 s delay. Cells had to exceed a peak firing rate of 2 Hz in at least one time bin to be considered active during the delay and to be included in the analysis. In addition, we computed correlations using time bins after splitting the delay lengths (10 s and

60 s) into 5 s intervals. Finally, we examined whether time cells are coding for relative or absolute timing (MacDonald et al., 2011) across the two different delay conditions. To test for absolute timing, we performed a correlation between each time bin in the 10 s delay and the time bins over the first 10 s of the 60 s delay. To test for relative timing, we compressed the data over the 60 s delay into the same number of bins as in the 10 s delay condition and performed correlations between the two sets of time bins.

Linear classifier—To evaluate whether the population activity during the delay contained any information about trial type, we constructed population vectors in time intervals of 1 s length and z-scored them cell-wise using mean and standard deviation over time bins. Z-scored population vectors were then randomly divided into a training and a test set for a linear classifier (MATLAB's svm_train) to distinguish left and right turns within each 10 s interval of the 60 s delay period. We also trained 100 classifiers on the same data with randomly shuffled turn labels (left or right). We compared the left-right prediction from the classifier (correct classification rate, CCR) between real and shuffled data in two ways. First, we took the proportion of sessions in which the CCR from the real data was in the upper 95% quantile of the shuffled data. Second, we computed the z score of the CCR with respect to the shuffle distribution of CCRs. Moreover, we performed the classification in two ways, one in which we assigned left/right labels from the future turn direction and one in which we assigned the labels from the past turn direction. For only the analysis using the linear classifier, but not for other analyses in the manuscript, we included correct and incorrect trials because there was otherwise not a sufficient number of trials in the mEC lesioned animals to perform the analysis.

Spatial information—The information score describes the information density per spike and was calculated as described by (Skaggs et al., 1996),

$$I = \sum_{i=1}^{N} p_i \frac{\lambda_i}{\lambda} log_2 \frac{\lambda_i}{\lambda}$$

where I is the information density measured in bits per spike, i is the index of the pixels of the place field, p_i is the probability of the rat being at location i, λ_i is the average firing rate of the cell when the rat is at location i, and λ is the total average firing rate.

Rate differences on the stem and during the delay—Rate differences between correct trials with an upcoming left-turn or an upcoming right-turn were calculated by subtracting the average firing rate of each cell in left-turn trials from the rate in right-turn trials and by dividing the difference by the sum of the rates for both trial types. A two-fold rate difference (score: 0.33) was taken as the minimum criterion to consider a cell's firing distinct between trial types. Only correct trials were analyzed.

Shuffling procedures—To generate distributions that are shuffled in space, we shifted the spatial firing patterns on the two sides of the maze with respect to each other by random distances that were at least 10 spatial bins apart. This shuffling procedure retains the spatial distributions of activity patterns but not the correspondence between matching positions.

Using the shuffled data, we calculated both the trial by trial spatial correlations between the same trial type and the left versus right spatial correlations as above. For rate differences, shuffling by trial-type was preformed to determine whether rate differences on the stem and during the delays were trial-type dependent.

Statistical Analysis—Two-way ANOVAs were used to analyze behavioral data (Group x Delay) and sequence firing (Trial type x Block). Tukey's and Sidak multiple comparisons tests were used to analyze interactions. Linear regressions were used to analyze improvement in WM performance and to determine the extent to which the degree of mEC and parasubiculum damage was related to behavioral performance. Kolmogorov-Smirnov (KS) tests were performed to analyze differences between distributions, Mann-Whitney tests for between-group comparisons, and Wilcoxon tests for one-sample comparisons. Chi square tests were used to test whether observed fractions of active cells differed from the expected fractions.

Supplementary Material

Refer to Web version on PubMed Central for supplementary material.

Acknowledgements

REFERENCES

Aggleton JP, Hunt PR, and Rawlins JN (1986). The effects of hippocampal lesions upon spatial and non-spatial tests of working memory. Behav Brain Res 19, 133–146. [PubMed: 3964405]

Ainge JA, van der Meer MA, Langston RF, and Wood ER (2007). Exploring the role of context-dependent hippocampal activity in spatial alternation behavior. Hippocampus 17, 988–1002. [PubMed: 17554771]

Allen TA, Salz DM, McKenzie S, and Fortin NJ (2016). Nonspatial Sequence Coding in CA1 Neurons. J Neurosci 36, 1547–1563. [PubMed: 26843637]

Baeg EH, Kim YB, Huh K, Mook-Jung I, Kim HT, and Jung MW (2003). Dynamics of population code for working memory in the prefrontal cortex. Neuron 40, 177–188. [PubMed: 14527442]

Barak O, and Tsodyks M (2014). Working models of working memory. Curr Opin Neurobiol 25, 20–24. [PubMed: 24709596]

Bower MR, Euston DR, and McNaughton BL (2005). Sequential-context-dependent hippocampal activity is not necessary to learn sequences with repeated elements. J Neurosci 25, 1313–1323. [PubMed: 15703385]

Bragin A, Jando G, Nadasdy Z, Hetke J, Wise K, and Buzsaki G (1995). Gamma (40–100 Hz) oscillation in the hippocampus of the behaving rat. J Neurosci 15, 47–60. [PubMed: 7823151]

Buzsaki G, and Moser EI (2013). Memory, navigation and theta rhythm in the hippocampal-entorhinal system. Nat Neurosci 16, 130–138. [PubMed: 23354386]

Clark RE, Broadbent NJ, Zola SM, and Squire LR (2002). Anterograde amnesia and temporally graded retrograde amnesia for a nonspatial memory task after lesions of hippocampus and subiculum. J Neurosci 22, 4663–4669. [PubMed: 12040072]

Clark RE, Zola SM, and Squire LR (2000). Impaired recognition memory in rats after damage to the hippocampus. J Neurosci 20, 8853–8860. [PubMed: 11102494]

Csicsvari J, Hirase H, Czurko A, Mamiya A, and Buzsaki G (1999). Oscillatory coupling of hippocampal pyramidal cells and interneurons in the behaving Rat. J Neurosci 19, 274–287. [PubMed: 9870957]

de Lima MN, Luft T, Roesler R, and Schroder N (2006). Temporary inactivation reveals an essential role of the dorsal hippocampus in consolidation of object recognition memory. Neurosci Lett 405, 142–146. [PubMed: 16854527]

Diehl GW, Hon OJ, Leutgeb S, and Leutgeb JK (2017). Grid and Nongrid Cells in Medial Entorhinal Cortex Represent Spatial Location and Environmental Features with Complementary Coding Schemes. Neuron 94, 83–92 e86. [PubMed: 28343867]

Druckmann S, and Chklovskii DB (2012). Neuronal circuits underlying persistent representations despite time varying activity. Curr Biol 22, 2095–2103. [PubMed: 23084992]

Dudchenko PA, Wood ER, and Eichenbaum H (2000). Neurotoxic hippocampal lesions have no effect on odor span and little effect on odor recognition memory but produce significant impairments on spatial span, recognition, and alternation. J Neurosci 20, 2964–2977. [PubMed: 10751449]

Duva CA, Floresco SB, Wunderlich GR, Lao TL, Pinel JP, and Phillips AG (1997). Disruption of spatial but not object-recognition memory by neurotoxic lesions of the dorsal hippocampus in rats. Behav Neurosci 111, 1184–1196. [PubMed: 9438788]

Eichenbaum H (2014). Time cells in the hippocampus: a new dimension for mapping memories. Nat Rev Neurosci 15, 732–744. [PubMed: 25269553]

Ferbinteanu J, and Shapiro ML (2003). Prospective and retrospective memory coding in the hippocampus. Neuron 40, 1227–1239. [PubMed: 14687555]

Fernandez-Ruiz A, Oliva A, Nagy GA, Maurer AP, Berenyi A, and Buzsaki G (2017). Entorhinal-CA3 Dual-Input Control of Spike Timing in the Hippocampus by Theta-Gamma Coupling. Neuron 93, 1213–1226 e1215. [PubMed: 28279355]

Frank LM, Brown EN, and Wilson M (2000). Trajectory encoding in the hippocampus and entorhinal cortex. Neuron 27, 169–178. [PubMed: 10939340]

Fujisawa S, Amarasingham A, Harrison MT, and Buzsaki G (2008). Behavior-dependent short-term assembly dynamics in the medial prefrontal cortex. Nat Neurosci 11, 823–833. [PubMed: 18516033]

Fuster JM, and Alexander GE (1971). Neuron activity related to short-term memory. Science 173, 652–654. [PubMed: 4998337]

Gill PR, Mizumori SJ, and Smith DM (2011). Hippocampal episode fields develop with learning. Hippocampus 21, 1240–1249. [PubMed: 20665593]

Girardeau G, Benchenane K, Wiener SI, Buzsaki G, and Zugaro MB (2009). Selective suppression of hippocampal ripples impairs spatial memory. Nat Neurosci 12, 1222–1223. [PubMed: 19749750]

Griffin AL, Eichenbaum H, and Hasselmo ME (2007). Spatial representations of hippocampal CA1 neurons are modulated by behavioral context in a hippocampus-dependent memory task. J Neurosci 27, 2416–2423. [PubMed: 17329440]

Hafting T, Fyhn M, Molden S, Moser MB, and Moser EI (2005). Microstructure of a spatial map in the entorhinal cortex. Nature 436, 801–806. [PubMed: 15965463]

Hales JB, Schlesiger MI, Leutgeb JK, Squire LR, Leutgeb S, and Clark RE (2014). Medial entorhinal cortex lesions only partially disrupt hippocampal place cells and hippocampus-dependent place memory. Cell Rep 9, 893–901. [PubMed: 25437546]

Hales JB, Vincze JL, Reitz NT, Ocampo AC, Leutgeb S, and Clark RE (2018). Recent and remote retrograde memory deficit in rats with medial entorhinal cortex lesions. Neurobiol Learn Mem 155, 157–163. [PubMed: 30075194]

Hammond RS, Tull LE, and Stackman RW (2004). On the delay-dependent involvement of the hippocampus in object recognition memory. Neurobiol Learn Mem 82, 26–34. [PubMed: 15183168]

Hargreaves EL, Rao G, Lee I, and Knierim JJ (2005). Major dissociation between medial and lateral entorhinal input to dorsal hippocampus. Science 308, 1792–1794 [PubMed: 15961670]

Henze DA, Borhegyi Z, Csicsvari J, Mamiya A, Harris KD, and Buzsaki G (2000). Intracellular features predicted by extracellular recordings in the hippocampus in vivo. J Neurophysiol 84, 390–400. [PubMed: 10899213]

Heys JG, and Dombeck DA (2018). Evidence for a subcircuit in medial entorhinal cortex representing elapsed time during immobility. Nat Neurosci 21, 1574–1582. [PubMed: 30349104]

Hölscher C, Jacob W, and Mallot H (2004). Learned association of allocentric and egocentric information in the hippocampus. Experimental brain research 158.

Ito HT, Zhang SJ, Witter MP, Moser EI, and Moser MB (2015). A prefrontal-thalamo-hippocampal circuit for goal-directed spatial navigation. Nature 522, 50–55. [PubMed: 26017312]

Jadhav Shantanu P., Rothschild G, Roumis Demetris K., and Frank Loren M. (2016). Coordinated Excitation and Inhibition of Prefrontal Ensembles during Awake Hippocampal Sharp-Wave Ripple Events. Neuron 90, 113–127. [PubMed: 26971950]

Johnson A, and Redish AD (2007). Neural ensembles in CA3 transiently encode paths forward of the animal at a decision point. J Neurosci 27, 12176–12189. [PubMed: 17989284]

Kitamura T, Macdonald CJ, and Tonegawa S (2015). Entorhinal-hippocampal neuronal circuits bridge temporally discontiguous events. Learn Mem 22, 1549–5485

Koenig J, Linder AN, Leutgeb JK, and Leutgeb S (2011). The spatial periodicity of grid cells is not sustained during reduced theta oscillations. Science 332, 592–595. [PubMed: 21527713]

Kraus BJ, Brandon MP, Robinson RJ 2nd, Connerney MA, Hasselmo ME, and Eichenbaum H (2015). During Running in Place, Grid Cells Integrate Elapsed Time and Distance Run. Neuron 88, 578–589. [PubMed: 26539893]

Lee I, Griffin AL, Zilli EA, Eichenbaum H, and Hasselmo ME (2006). Gradual translocation of spatial correlates of neuronal firing in the hippocampus toward prospective reward locations. Neuron 51, 639–650. [PubMed: 16950161]

Lee I, and Kesner RP (2003). Time-dependent relationship between the dorsal hippocampus and the prefrontal cortex in spatial memory. J Neurosci 23, 1517–1523. [PubMed: 12598640]

Liu D, Gu X, Zhu J, Zhang X, Han Z, Yan W, Cheng Q, Hao J, Fan H, Hou R, et al. (2014). Medial prefrontal activity during delay period contributes to learning of a working memory task. Science 346, 458–463. [PubMed: 25342800]

MacDonald CJ, Lepage KQ, Eden UT, and Eichenbaum H (2011). Hippocampal "time cells" bridge the gap in memory for discontiguous events. Neuron 71, 737–749. [PubMed: 21867888]

Mankin EA, Sparks FT, Slayyeh B, Sutherland RJ, Leutgeb S, and Leutgeb JK (2012). Neuronal code for extended time in the hippocampus. Proc Natl Acad Sci U S A 109, 19462–19467. [PubMed: 23132944]

McKenzie S, Frank AJ, Kinsky NR, Porter B, Riviere PD, and Eichenbaum H (2014). Hippocampal representation of related and opposing memories develop within distinct, hierarchically organized neural schemas. Neuron 83, 202–215. [PubMed: 24910078]

Miao C, Cao Q, Ito HT, Yamahachi H, Witter MP, Moser MB, and Moser EI (2015). Hippocampal Remapping after Partial Inactivation of the Medial Entorhinal Cortex. Neuron 88, 590–603. [PubMed: 26539894]

Miller VM, and Best PJ (1980). Spatial correlates of hippocampal unit activity are altered by lesions of the fornix and endorhinal cortex. Brain Res 194, 311–323. [PubMed: 7388617]

Mongillo G, Barak O, and Tsodyks M (2008). Synaptic theory of working memory. Science 319, 1543–1546. [PubMed: 18339943]

Mumby DG, Wood ER, Duva CA, Kornecook TJ, Pinel JP, and Phillips AG (1996). Ischemia-induced object-recognition deficits in rats are attenuated by hippocampal ablation before or soon after ischemia. Behav Neurosci 110, 266–281. [PubMed: 8731053]

Newman EL, and Hasselmo ME (2014). CA3 sees the big picture while dentate gyrus splits hairs. Neuron 81, 226–228. [PubMed: 24462091]

O'Reilly KC, Alarcon JM, and Ferbinteanu J (2014). Relative contributions of CA3 and medial entorhinal cortex to memory in rats. Front Behav Neurosci 8, 292. [PubMed: 25221487]

Olton DS, Becker JT, Handelmann GE (1979). Hippocampus, space, and memory. Behavioral and Brain Sciences 2 313–322.

Pastalkova E, Itskov V, Amarasingham A, and Buzsaki G (2008). Internally generated cell assembly sequences in the rat hippocampus. Science 321, 1322–1327. [PubMed: 18772431]

Perez-Escobar JA, Kornienko O, Latuske P, Kohler L, and Allen K (2016). Visual landmarks sharpen grid cell metric and confer context specificity to neurons of the medial entorhinal cortex. Elife 5 %! Visual landmarks sharpen grid cell metric and confer context specificity to neurons of the medial entorhinal cortex %@ 2050–084X (Electronic) 2050–084X (Linking).

Pfeiffer BE, and Foster DJ (2013). Hippocampal place-cell sequences depict future paths to remembered goals. Nature 497, 74–79. [PubMed: 23594744]

Prusky GT, Douglas RM, Nelson L, Shabanpoor A, and Sutherland RJ (2004). Visual memory task for rats reveals an essential role for hippocampus and perirhinal cortex. Proc Natl Acad Sci U S A 101, 5064–5068. [PubMed: 15051876]

Rampon C, Tang YP, Goodhouse J, Shimizu E, Kyin M, and Tsien JZ (2000). Enrichment induces structural changes and recovery from nonspatial memory deficits in CA1 NMDAR1-knockout mice. Nat Neurosci 3, 238–244. [PubMed: 10700255]

Robinson NTM, Priestley JB, Rueckemann JW, Garcia AD, Smeglin VA, Marino FA, and Eichenbaum H (2017). Medial Entorhinal Cortex Selectively Supports Temporal Coding by Hippocampal Neurons. Neuron 94, 677–688 e676. [PubMed: 28434800]

Rueckemann JW, DiMauro AJ, Rangel LM, Han X, Boyden ES, and Eichenbaum H (2016). Transient optogenetic inactivation of the medial entorhinal cortex biases the active population of hippocampal neurons. Hippocampus 26, 246–260. [PubMed: 26299904]

Salz DM, Tiganj Z, Khasnabish S, Kohley A, Sheehan D, Howard MW, and Eichenbaum H (2016). Time Cells in Hippocampal Area CA3. J Neurosci 36, 7476–7484. [PubMed: 27413157]

Sasaki T, Piatti VC, Hwaun E, Ahmadi S, Lisman JE, Leutgeb S, and Leutgeb JK (2018). Dentate network activity is necessary for spatial working memory by supporting CA3 sharp-wave ripple generation and prospective firing of CA3 neurons. Nat Neurosci 21, 258–269. [PubMed: 29335604]

Schlesiger MI, Boublil BL, Hales JB, Leutgeb JK, and Leutgeb S (2018). Hippocampal Global Remapping Can Occur without Input from the Medial Entorhinal Cortex. Cell Rep 22, 3152–3159. [PubMed: 29562172]

Schlesiger MI, Cannova CC, Boublil BL, Hales JB, Mankin EA, Brandon MP, Leutgeb JK, Leibold C, and Leutgeb S (2015). The medial entorhinal cortex is necessary for temporal organization of hippocampal neuronal activity. Nat Neurosci 18, 1123–1132. [PubMed: 26120964]

Shapiro ML, and Eichenbaum H (1999). Hippocampus as a memory map: synaptic plasticity and memory encoding by hippocampal neurons. Hippocampus 9, 365–384. [PubMed: 10495019]

Singer AC, Karlsson MP, Nathe AR, Carr MF, and Frank LM (2010). Experience-dependent development of coordinated hippocampal spatial activity representing the similarity of related locations. J Neurosci 30, 11586–11604. [PubMed: 20810880]

Skaggs WE, McNaughton BL, Wilson MA, and Barnes CA (1996). Theta phase precession in hippocampal neuronal populations and the compression of temporal sequences. Hippocampus 6, 149–172. [PubMed: 8797016]

Smith DM, and Mizumori SJ (2006). Learning-related development of context-specific neuronal responses to places and events: the hippocampal role in context processing. J Neurosci 26, 3154–3163 [PubMed: 16554466]

Stokes MG (2015). 'Activity-silent' working memory in prefrontal cortex: a dynamic coding framework. Trends Cogn Sci 19, 394–405. [PubMed: 26051384]

Suh J, Rivest AJ, Nakashiba T, Tominaga T, and Tonegawa S (2011). Entorhinal cortex layer III input to the hippocampus is crucial for temporal association memory. Science 334, 1415–1420 [PubMed: 22052975]

Takehara K, Kawahara S, and Kirino Y (2003). Time-dependent reorganization of the brain components underlying memory retention in trace eyeblink conditioning. J Neurosci 23, 9897–9905. [PubMed: 14586019]

Tiganj Z, Jung MW, Kim J, and Howard MW (2017). Sequential Firing Codes for Time in Rodent Medial Prefrontal Cortex. Cereb Cortex 27, 5663–5671. [PubMed: 29145670]

Wood ER, Dudchenko PA, Robitsek RJ, and Eichenbaum H (2000). Hippocampal neurons encode information about different types of memory episodes occurring in the same location. Neuron 27, 623–633. [PubMed: 11055443]
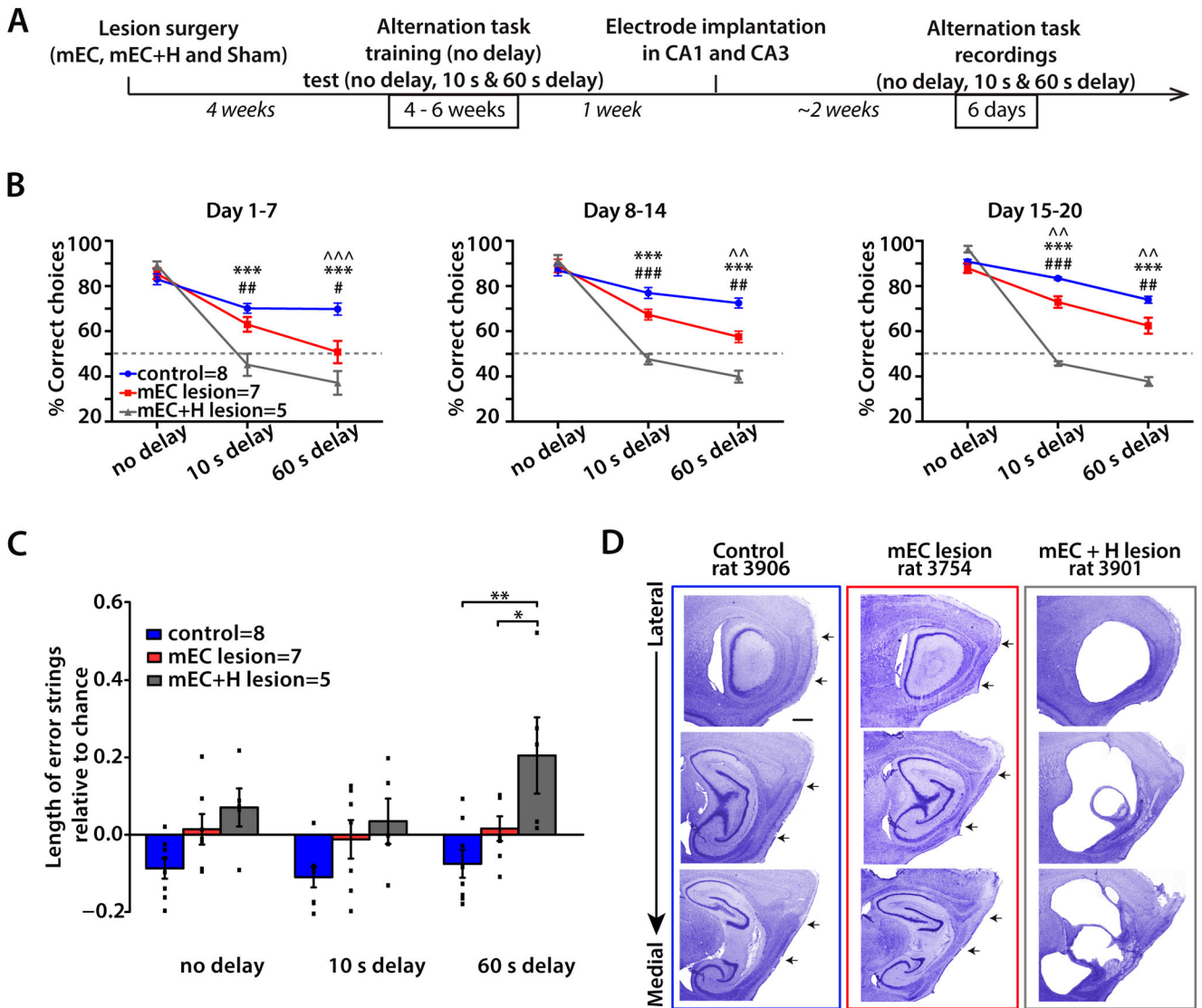
Yang ST, Shi Y, Wang Q, Peng JY, and Li BM (2014). Neuronal representation of working memory in the medial prefrontal cortex of rats. Mol Brain 7, 61. [PubMed: 25159295]

Zheng C, Bieri KW, Hsiao YT, and Colgin LL (2016). Spatial Sequence Coding Differs during Slow and Fast Gamma Rhythms in the Hippocampus. Neuron 89, 398–408. [PubMed: 26774162]

Figure 1. WM performance was impaired in mEC lesioned rats.

(A) Experimental timeline. Rats underwent mEC lesions, combined mEC+H lesions, or sham surgeries (control) and were then trained in a spatial alternation task, first with only no delay trials and later with blocks of 10 s and 60 s delay trials included on each day. Tetrodes were implanted after 14 days of behavioral training with all delay conditions, and at least six days of recordings in the WM task were performed after tetrodes were positioned in CA1 and CA3. (B) Behavioral performance in the alternation task. MEC-lesioned and mEC+H-lesioned rats were impaired in the delayed versions but not in the continuous version of the task. The 20 days of testing were analyzed in three blocks (7 days, 7 days, and 6 days). Two-way ANOVAs (Group x Delay) for each of the three blocks revealed main effects of Lesion and Delay and a Delay x Lesion interaction (see Table S1). Tukey's posthoc tests: ^^ p < 0.01, ^^^ p < 0.001 for control vs. mEC lesion group comparisons, *** p < 0.001 for control vs. mEC+H lesion group comparisons, and # p < 0.05, ## p < 0.01, ### p < 0.001 for mEC vs. mEC+H lesion group comparisons. (C) Length of error strings relative to chance. Given

the number of errors committed by the animals in each group and condition, the average number of consecutive errors that would be expected by chance was calculated by shuffling these data 100 times and by then subtracting the shuffled values from the average number of consecutive errors observed. A two-way ANOVA (Group x Delay) revealed a significant effect of Group (p = 0.0029), and the differences between groups were in the 60 s delay condition where the combined lesion group made significantly more consecutive errors than both the control group and the mEC lesion group (** p = 0.0002 and * p = 0.019, Tukey's test). (D) Series of sagittal sections from a control (left), an mEC-lesioned (middle), and an mEC+H lesioned (right) rat. Scale bar = 500 μm. Arrows indicate the dorsal and ventral borders of mEC. See also Figure S1, S2, S3, Table S1 and S3.
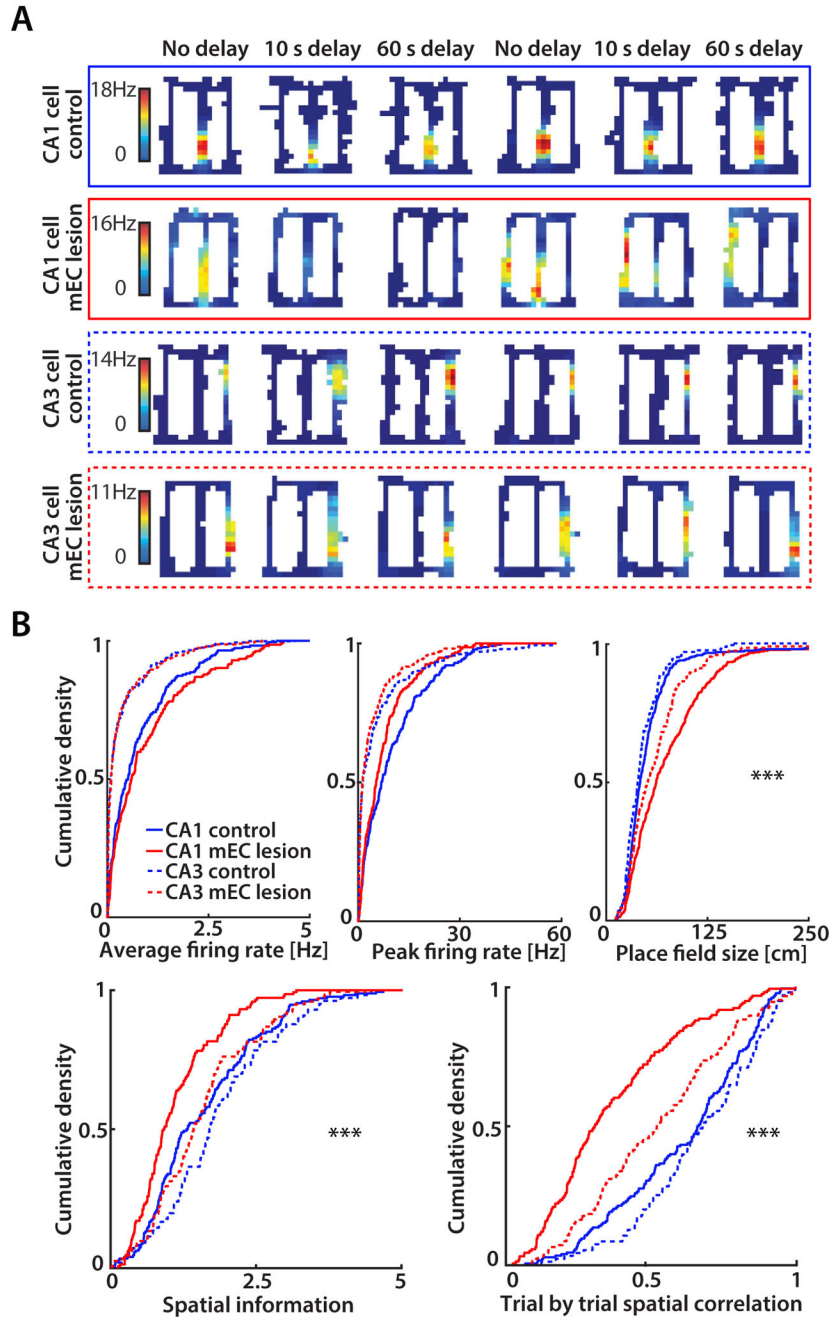
Figure 2. MEC lesions had a larger effect on field size, spatial precision and stability in CA1 compared to CA3.

(A) Rate maps of CA1 and CA3 cells. Each row is a cell's firing pattern for each of the 6 blocks (two per delay condition). CA1 place fields were unstable and changed firing location in mEC-lesioned rats. Color bars indicate the firing rate (from 0 Hz in blue to the peak rate in all blocks in red). (B) Cumulative density functions (CDFs) of average firing rate, peak firing rate, field size, spatial information, and trial-by-trial spatial correlation. Average firing rates and peak firing rates were not different between control and mEC lesion groups in either CA1 (mEC n = 233 cells, control n = 246 cells; n.s., KS test) or CA3 (mEC n = 359

cells, control n = 218 cells; n.s., KS test). CA1 and CA3 place fields were larger in the mEC lesion group compared to controls (p < 0.0001, KS test) with a larger effect on CA1 than CA3 place field size in mEC lesioned rats (two-way ANOVA with Lesion x Hippocampal subfield as factors; posthoc analysis, Tukey's test: differences between CA1 and CA3 in the control group, n.s., in the mEC lesion group, *** p < 0.0001). Spatial information for cells active on the maze (peak firing > 2 Hz) was different between control and mEC lesion groups in CA1 (mEC n = 158 cells, control n = 178 cells; *** p < 0.0001, KS test), but not CA3 (n = 143 cells, control n = 96 cells; n.s., KS test). Trial-by-trial spatial correlation (i.e., spatial stability) for cells active on the maze was lower in the mEC lesion compared to the control group in both CA1 and CA3 (*** p < 0.0001, KS tests). The effect on spatial stability was larger in CA1 compared to CA3 in mEC-lesioned rats (two-way ANOVA with Lesion and Hippocampal subfield as factors; posthoc analysis, Tukey's test: spatial stability differed between every combination of subfield and lesion, all p values < 0.001, except between control CA1 and control CA3). See also Figure S1.
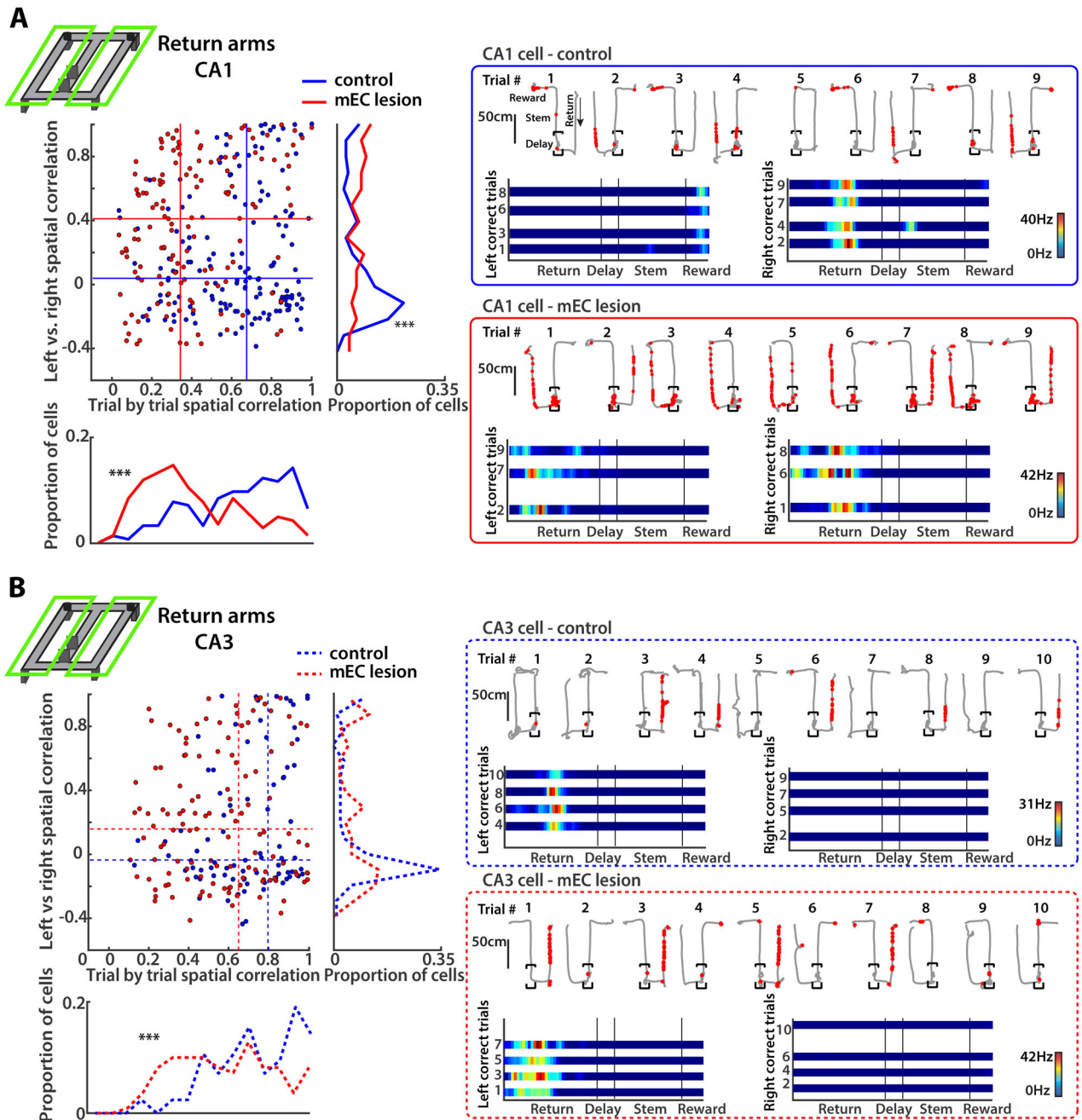
**Figure 3. MEC lesions impaired spatial coding on the return arms to a larger extent in CA1 than in CA3**

(A) (Left) Spatial correlation between the average firing pattern on left compared to right maze segments (left vs. right, vertical axis) and, as a measure of place field stability, between single trials with the same turn direction (trial-by-trial, horizontal axis). Only correct trials were used for the analysis, and each dot in the scatterplot is a CA1 cell. Data for each type of spatial correlation are summarized in histograms to the right and on the bottom (*** p < 0.0001, KS test). The median values of each group (control and mEC lesion) are shown as horizontal and vertical lines within the scatterplot. (Right) Example

CA1 cells from a control and an mEC-lesioned rat. Top row of each example are single correct and incorrect trials (path in grey, spike locations as red dots), and bottom row are linearized rate maps of correct left and correct right trials. Color bars indicate the firing rate (from 0 Hz in blue to the peak rate in all trials in red). (B) Same as A, but for CA3 cells. A larger number of CA3 compared to CA1 cells in mEC-lesioned rats were stable from trial to trial and discriminated between right and left maze segments. See also Figure S4.
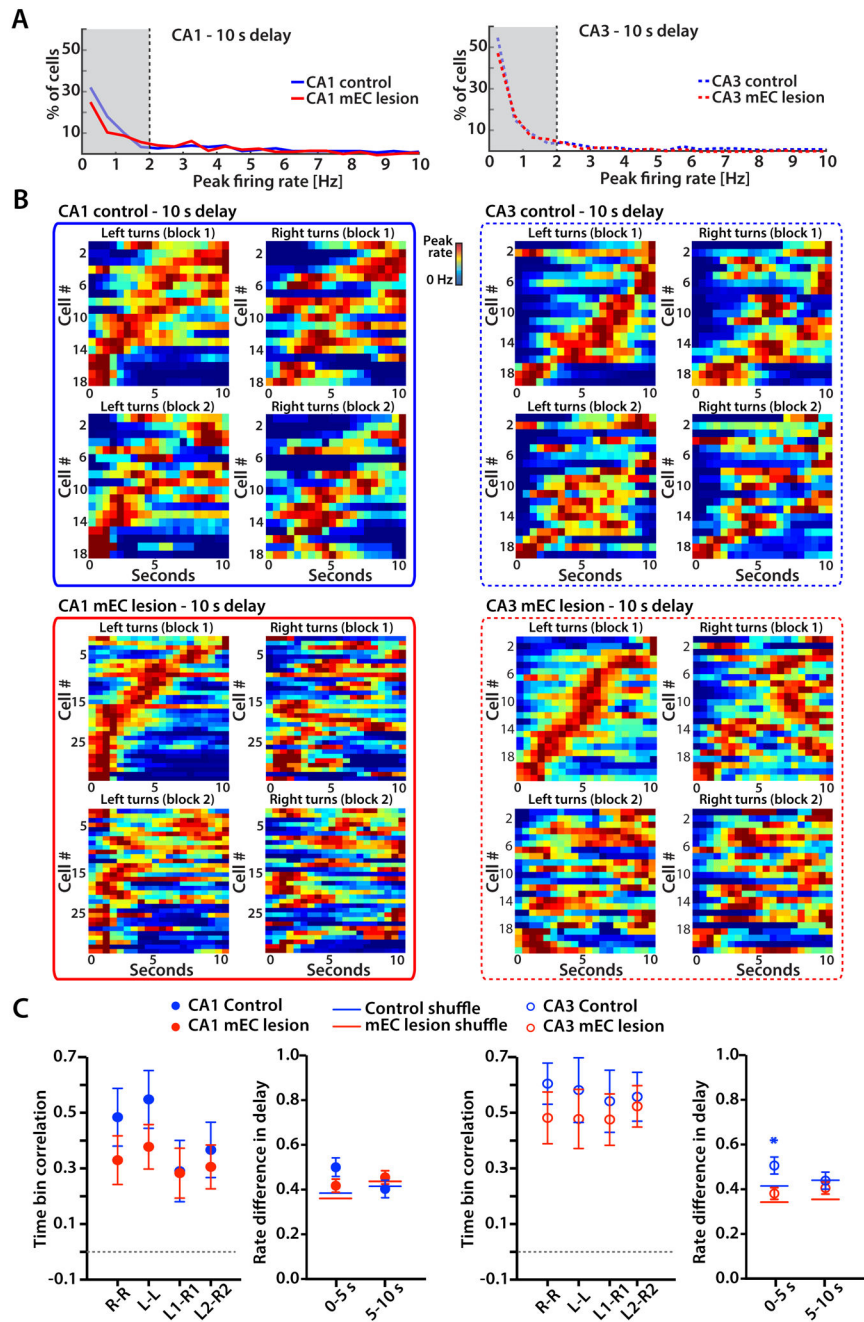
Figure 4. Time cells during the 10 s delay period did not distinguish between left-turn and right-turn trials in either control or mEC-lesioned rats

(A) For each cell, firing rates were calculated for 500 ms bins throughout the 10 s delay interval of correct trials. The distribution of peak firing rates from all CA1 cells (left) and CA3 cells (right) from control and mEC lesioned rats is shown. Cells with peak rates > 2 Hz in at least one time bin were considered active during the delay. (B) Temporal firing patterns of all CA1 cells and CA3 cells that were active during the 10 s delay. Each row is the average firing rate for a single cell over one block, normalized to the cell's peak rate. Cells are sorted by the time of the peak during the first block of left-turn trials. Color bars indicate

the firing rate from 0 Hz in blue to the peak rate in red. (C) For each cell, the correlation between corresponding time bins over the 10 s delay (i.e., time bin correlation) was calculated between left-turn and right-turn trials within a block and between trials of the same type across the two blocks (n.s., two-way ANOVA with trial type and blocks as factors). Symbols and error bars are the mean ± SEM. Left versus right rate differences in delay were also calculated using 5 s increments (* $p < 0.05$, Mann-Whitney test). See also Figure S5 and Table S4.
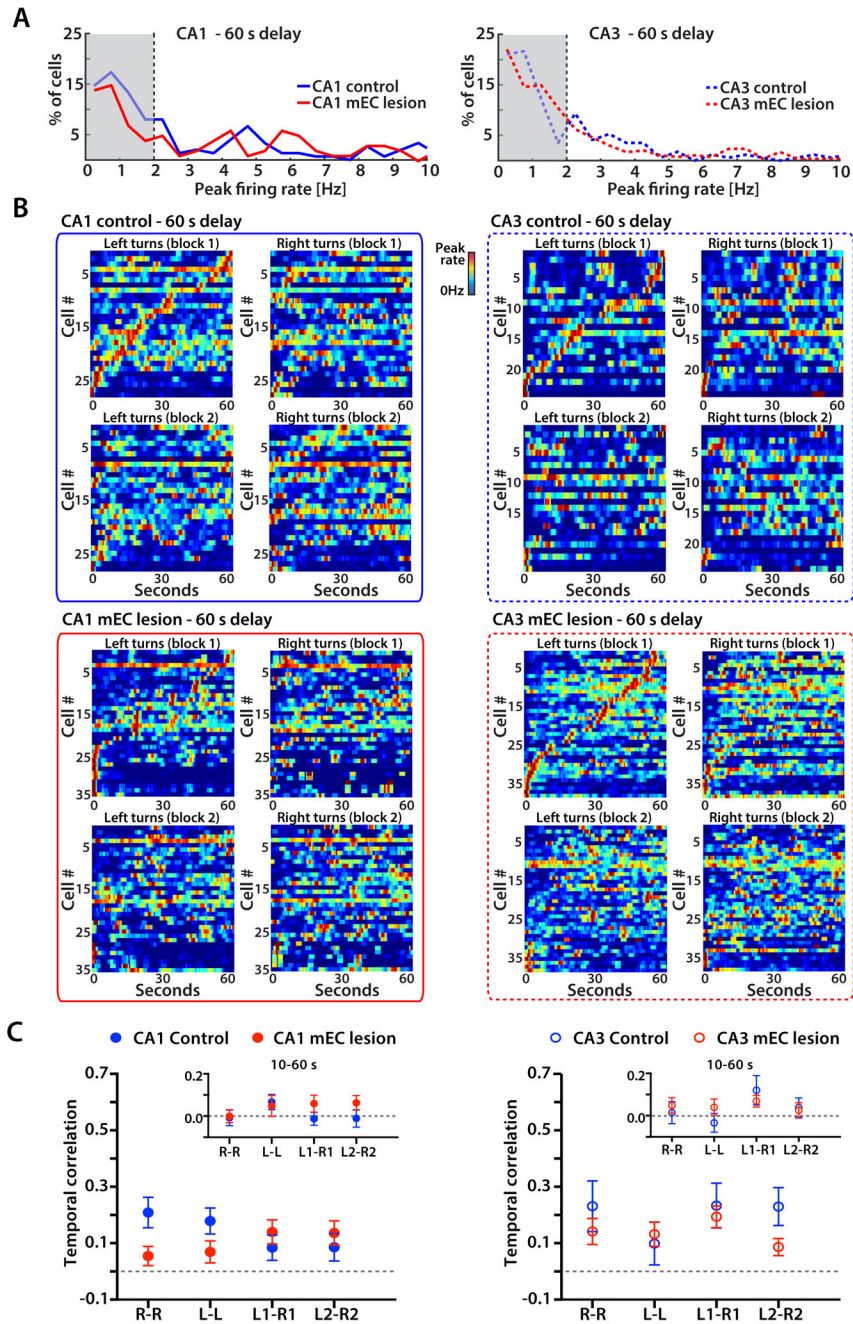
Figure 5. Time cells do not bridge discontinuous events over 60 s retention intervals
(A) For each cell, firing rates were calculated for each 500 ms bin throughout the 60 s delay interval of correct trials, and the distribution of peak firing rates from all CA1 (left) and CA3 (right) cells from control and mEC lesioned rats is shown. (B) Temporal firing patterns of all CA1 cells and CA3 cells that were active during the 60 s delay. Each row is the average firing rate for a single cell over one block, normalized by the cell's peak rate. Cells are sorted by the time of the peak during the first block of left-turn trials. Color bars indicate the firing rate from 0 Hz in blue to the peak rate in red. (C) For each cell, the correlation between corresponding time bins over the 60 s delay (i.e., temporal correlation) was
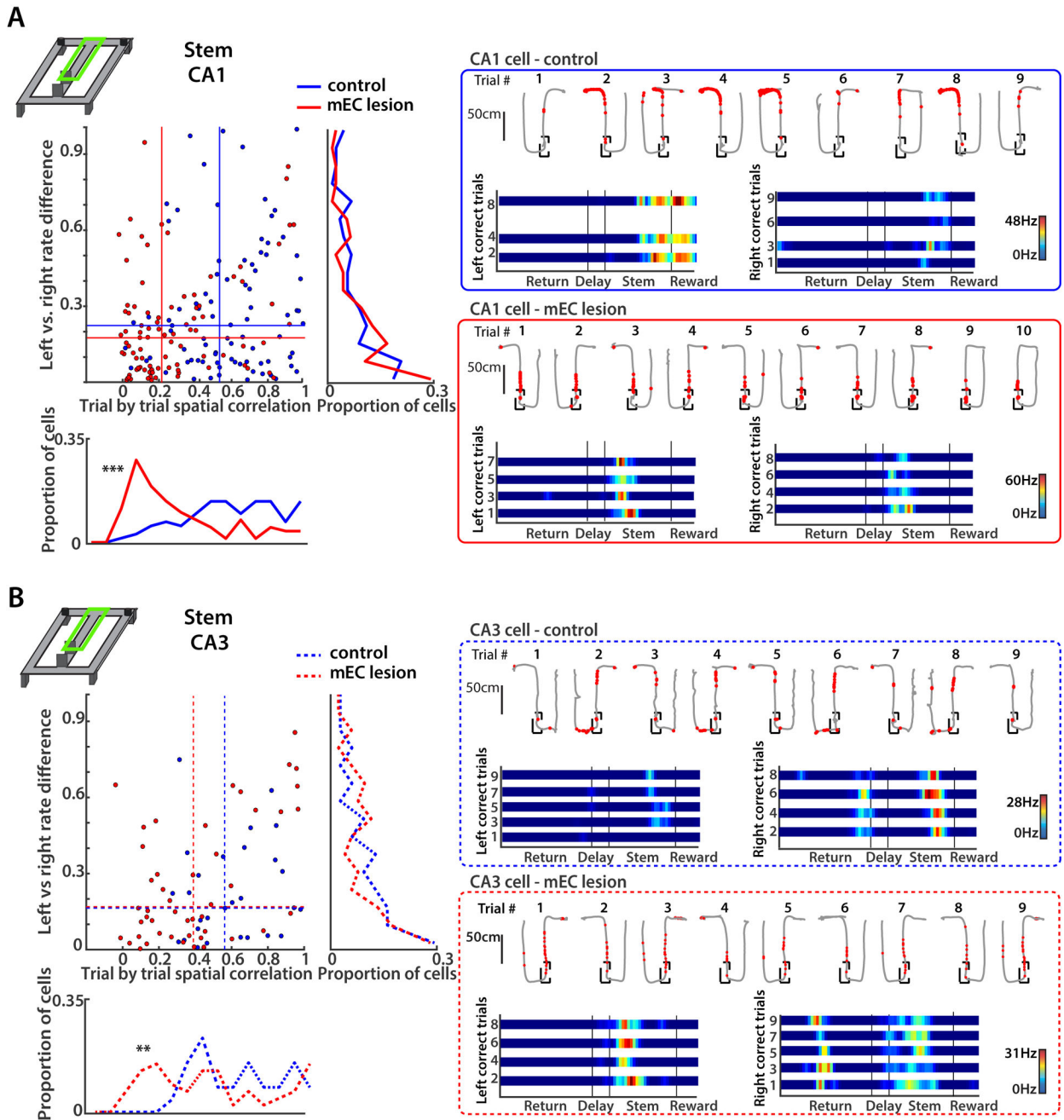
calculated between left-turn and right-turn trials within a block and between trials of the same type across the two blocks (n.s., two-way ANOVA with Trial type and Blocks as factors). Symbols and error bars are the mean ± SEM. Insets: cell-by-cell temporal correlation between blocks and trial types, excluding the first 10 s of the 60 s delay interval (n.s., two-way ANOVA). See also Figures S5, S6 and Table S4.
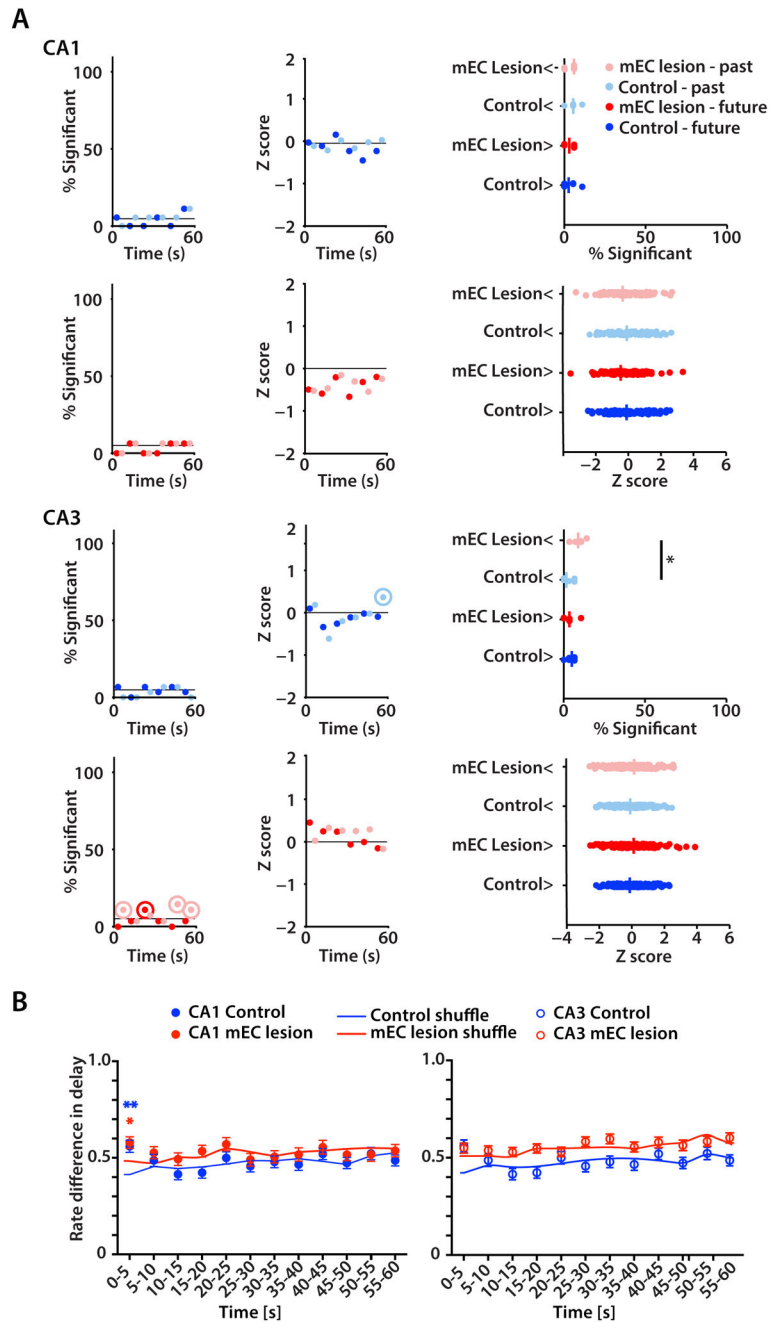
Figure 6. Trial type could not be decoded with a linear classifier nor from rate differences past the first 5 s of the 60 s delay

(A) Left: Fraction of sessions in which the correct classification rate (CCR) from the real data was in the upper 95% quantile of the shuffles. Analysis was done for 1 s long population vectors within each 10 s time segment of the 60 s delay and by using either upcoming turn direction (dark colors) or previous turn direction (light colors). Dots in circles indicate significance using a Binomial test, $p < 0.05$. Middle: Median Z score of CCRs within each 10 s interval. Z scores were calculated by comparing real CCR values to distributions for which the trial-type label was shuffled. Dots within circles indicate

significance using a Wilcoxon test, p < 0.05. Right: Summary indicating significant differences between groups for % significant (* p < 0.05, Mann-Whitney test) and differences from zero for Z scores (all n.s., Wilcoxon test). (B) Left versus right rate differences during delay were calculated using 5 s time segments. The differences calculated from real data were compared to rate differences from data shuffled by trial type. Rate differences were only informative about trial type in CA1 during the first 5 s (* p < 0.05, ** p < 0.01, Mann-Whitney test).

Figure 7. Trajectory-dependent firing in the stem was not reduced by mEC lesions for either CA1 or CA3 cells.

(A) Left: CA1 rate difference between correct left-turn and right-turn trials (left vs. right, vertical axis), and spatial correlation between single trials with the same turn direction (trial-by-trial, horizontal axis). Data for the trial-wise spatial correlations are summarized in the histogram on the bottom (trial-by-trial, ***p < 0.0001, KS test), and data for the rate differences are summarized to the right (left vs. right rate difference, n.s., KS test). The median values of each group (control and mEC lesion) are shown as horizontal and vertical lines within the scatterplot. Right: Example CA1 cells from a control and an mEC-lesioned

rat. Top row of each example are single correct and incorrect trials (path in grey, spike locations as red dots) and bottom row are linearized rate maps of correct left and correct right trials. Color bars indicate the firing rate with 0 Hz in blue and the peak rate in all trials in red. Note that most cells with differential activity on the stem fire at corresponding locations across trials, but with higher rates in one trial type compared to the other. (B) Same as A, but for CA3 cells. In control and MEC-lesioned rats, similar proportions of CA1 and CA3 cells show differences in firing between correct left and right-turn trials. Trial-wise spatial correlations were decreased by the mEC lesion (bottom: ** $p < 0.01$, KS test). See also Figure S7 and Table S2.

KEY RESOURCES TABLE

REAGENT or RESOURCE	SOURCE	IDENTIFIER
Antibodies		
Biological Samples		
Chemicals, Peptides, and Recombinant Proteins		
Isoflurane	MWI	Cat #: NDC 13985-528-60
Buprenorphine	MWI	Cat #: 29308
Plantinic acid for platinum plating	Sigma-Aldrich	Cat #: 206083; CAS 18497-13-7
Sodium pentobarbital	MWI	Cat #: 15199
Formaldehyde	EMD	Cat #: FX-0415-4; CAS 50-00-0
NMDA	Tocris Bioscience	Cat #: 0114; CAS 6384-92-5
Ibotenic acid	Tocris Bioscience	Cat #: 0285; CAS 2552-55-8
Cresyl violet	EMD	Cat #: M-19012; CAS 10510-54-0
Critical Commercial Assays		
Deposited Data		
Experimental Models: Cell Lines		

REAGENT or RESOURCE	SOURCE	IDENTIFIER
Experimental Models: Organisms/Strains		
Long Evans rats	Charles River Labs	RRID: RGD_2308852
Recombinant DNA		
Sequence-Based Reagents		
Software and Algorithms		
MClust	A.D. Redish	http://redishlab.neuroscience.umn.edu/MClust/MClust.html
Matlab v 2015b	Mathworks	RRID: SCR_001622
Other		
Hyperdrive	Custom built; Designed by B McNaughton	US Patent: US5928143 A
Platinum-Iridium tetrode wire	California fine wire company	Cat #: CFW0011873
Freezing microtome	Leica	Model: SM 2000R
Digital Neuralynx recording system	Neuralynx	Model: Digital Lynx SX